

# Superheating effects during the melting of crystallites of syndiotactic polypropylene analysed by temperature-modulated differential scanning calorimetry

J. E. K. Schawe<sup>a,\*</sup> and G. R. Strobl<sup>b</sup>

<sup>a</sup>*Sektion für Kalorimetrie, Universität Ulm, 89069 Ulm, Germany*

<sup>b</sup>*Fakultät für Physik, Universität Freiburg, 79104 Freiburg, Germany*

(Received 3 September 1997; accepted 11 November 1997)

Temperature modulated differential scanning calorimetry (TMd.s.c.) was applied in a study of syndiotactic polypropylene. The crystallites melt from their lateral surfaces only and the kinetics shows up in the imaginary part  $c''$  of the complex specific heat. Theoretical analysis predicts and experiments confirm that  $c''$  increases linearly with the underlying mean heating rate and the modulation period. Furthermore, it can be shown that  $c''$  is inversely related to the superheating effective during melting. Use of the relation yields for syndiotactic polypropylene values in agreement with direct measurements employing conventional d.s.c. © 1998 Elsevier Science Ltd. All rights reserved.

(Keywords: polymer melting; temperature-modulated differential scanning calorimetry; syndiotactic polypropylene)

## INTRODUCTION

Crystallization of polymers leads to partially crystalline structures which are determined by both the thermodynamic conditions and the kinetics of transformation<sup>1,2</sup>. The latter is controlled by dynamic processes located around the growth faces of the layer-like crystallites, as given by the detachment and attachment of chain sequences, the transport of non-crystallizable chain parts into the adjacent amorphous regions (short chain branches, co-units, entanglements etc.) or, in the case of layer-by-layer growth, the formation of secondary nuclei. Being controlled by the kinetics, the partially crystalline state of polymers does not represent a stable equilibrium. Structure may continue to change with time, isothermally or during cooling. Correspondingly, the reverse process of melting is complex as well. Thermograms obtained by differential calorimetry represent in general a superposition of the melting of crystallites of different stability and exothermal recrystallization processes. Temperature-modulated differential scanning calorimetry (TMd.s.c.), which registers the sample response on small periodic temperature variations, can contribute to a discrimination<sup>3</sup>. In particular, it can be used to focus on the dynamic processes taking place at the growth faces. Work in this direction has started only recently, in experiments reported by Wunderlich *et al.*, Schick *et al.* and Toda *et al.* Employing a quasi-isothermal mode in a study on polyethylene terephthalate, Wunderlich and Okasaki deduced from the intensity of the periodic signal the fraction of crystallites undergoing at a given temperature a reversible local melting<sup>4</sup>. Schick and coworkers followed the same route in a study of PEEK<sup>5</sup>. Toda *et al.* show that the phase lag between sample temperature and heat flow depends on the temperature coefficient of the growth rate of

the crystallites and utilize the relation in studies of polyethylene<sup>6</sup> and polyethylene terephthalate<sup>7</sup>.

Recently we carried out a detailed investigation of the crystallization and melting behaviour of syndiotactic polypropylene (s-PP), using time- and temperature-dependent small-angle X-ray scattering experiments and calorimetry<sup>8</sup>. If s-PP is crystallized isothermally at temperatures above 120°C, it has a well-defined morphology, being composed of stacks of laterally extended lath-shaped crystallites with a uniform thickness in the range of 5–10 nm. The amorphous layers between the lamellae show a broad distribution with an average thickness around 15 nm. As for polymer crystals in general, so for s-PP melting takes place on the lateral crystal surfaces only. Therefore, crystals usually need a finite, comparatively long time for their melting. This is already indicated in conventional d.s.c.-runs by a shift of the melting peak which increases with the heating rate (in addition to the shift caused by heat transfer effects). In the following we shall show that this superheating may be studied in more detail by TMd.s.c.-measurements and will employ the relation in an evaluation of results obtained for s-PP.

## EXPERIMENTAL

The s-PP sample under study was synthesized by S. Jüngling in Professor Mülhaupt's group in the Institute of Macromolecular Chemistry of the University of Freiburg. The number average molecular weight  $M_n$  was  $1.04(10^5 \text{ g mol}^{-1})$  ( $M_w/M_n = 2.3$ ). More details on the sample properties are given in Ref. <sup>9</sup>.

For d.s.c. experiments a thin foil (90  $\mu\text{m}$ ) was pressed and put in a d.s.c. pan (sample mass: 4.94 mg). Before each measurement, samples were kept for some time in the melt at 165°C and then were quenched to the crystallization

\* To whom correspondence should be addressed

temperature, chosen at  $T_c = 130^\circ\text{C}$ . The crystallization time was 3 h. Conventional d.s.c. measurements conducted at 0.5 K/min indicated a direct melting with no signs of a recrystallization process. The TMD.s.c. measurements were carried out with a Perkin–Elmer DSC-7 in the DDSC mode. The input parameters ( $T_1$ ,  $T_2$ ,  $\beta_1$  and  $T_3$ ) were selected in such a way that the underlying heating rate  $\beta_0$ , the temperature amplitude  $T_a$  and the frequency  $f$  which follow from:

$$\beta_0 = \frac{\beta_1(T_3 - T_1)}{2(T_2 - T_1)} \quad (1a)$$

$$T_a = \frac{1}{2} \left( T_2 - \frac{T_1 - T_3}{2} \right) \quad (1b)$$

$$f = \frac{\beta_1}{2(T_2 - T_1)} \quad (1c)$$

had the desired values. Both the temperature program  $T(t)$  and the measured heat flow  $\Phi(t)$  represent a superposition of an underlying and a periodic component. By averaging over one period the underlying components result. The underlying component of the heat flow,  $\Phi_u$ , is identical with the signal in conventional d.s.c. runs. In the general case, where heats of reaction or transition may be included, it reads

$$\Phi_u = C_p \beta_0 + \Delta H_r \dot{\xi} = C_\beta \beta_0 \quad (2)$$

Here  $C_p$  is the ‘true heat capacity’, i.e. that associated with the equilibrium structure and dynamics of a given phase,  $\Delta H_r$  is the heat of reaction or transition, and  $\dot{\xi}$  denotes the reaction or transition rate;  $C_\beta$  denotes the ‘generalized heat capacity’ which may change with the underlying heating rate.

Fourier analysis yields the first harmonic of the periodic component,  $\Phi_{p1}$ . It reads

$$\Phi_{p1} = \omega T_{a1} |C| \cos(\omega t - \phi) = \omega T_{a1} (C' \cos(\omega t) + C'' \sin(\omega t)) \quad (3)$$

Here  $T_{a1}$  is the amplitude of the first harmonic of the temperature signal,  $\phi$  gives the phase shift between the first harmonic of the heating rate and the heat flow,  $|C|$  denotes the modulus of the complex heat capacity, and  $\omega$  equals  $2\pi f$ ;

$C'$  and  $C''$  are the real and the imaginary part of the complex heat capacity<sup>10</sup>. Calibration procedures have to be applied in order to obtain  $\Phi_{p1}$  correctly<sup>11,12</sup>.

## RESULTS AND DISCUSSION

### Check of linearity properties

A typical TMD.s.c. curve of s-PP is shown in *Figure 1*. In  $c_\beta$  ( $= C_\beta/m$ ;  $m$  is sample mass) the crystallite melting shows up. It starts immediately above the crystallization temperature, then increases in rate and reaches a maximum at  $152^\circ\text{C}$ . Melting becomes reflected also in the complex heat capacity.  $c'$  shows a small negative peak in the melting region.  $c''(T)$  has a similar shape to  $c_\beta$  and is always positive.

The melting of polymer crystallites may include non-linear effects. On the other hand, the data evaluation being based on a Fourier analysis considers only the linear response. Therefore, in order to minimize possible errors, the experimental conditions must be selected in such a way that the sample response is at least near to linear. We performed several checks.

First, we varied the sample mass and the amplitude of the temperature variation. The investigation of the influence of the sample mass on the measured signal is a method to clarify if the calibration procedure considers the heat transfer conditions into the sample correctly. We found that for sample masses in a range of 1–8 mg the  $c'$ - and  $c''$ -curves in the melting region remained unchanged. Variation of  $T_a$  also did not lead to any changes.

Next we looked at the shape of  $\Phi_p$ . In *Figure 2* both the heat flow  $\Phi(t)$  and the periodic component are shown. Ideally, the mean value of  $\Phi_p$  should be zero. Around  $153^\circ\text{C}$  one observes slight deviations. The reason is an error in the determination of the underlying signal. The relaxation of the heat flow at the end of the peak is relatively fast, too fast for the mathematical averaging procedure. The error is not serious since the effect on the amplitude of the periodic component appears negligible.

*Figure 3* depicts  $\Phi_p$  in higher resolution in two regions, around the melting peak ( $151^\circ\text{C}$ , lower curve) and in the melt ( $156^\circ\text{C}$ , upper curve). The periodic temperature variation has the form of a saw-tooth oscillation (linear heating and cooling). Consequently, a rectangular-shaped oscillation is expected for the corresponding heat flow

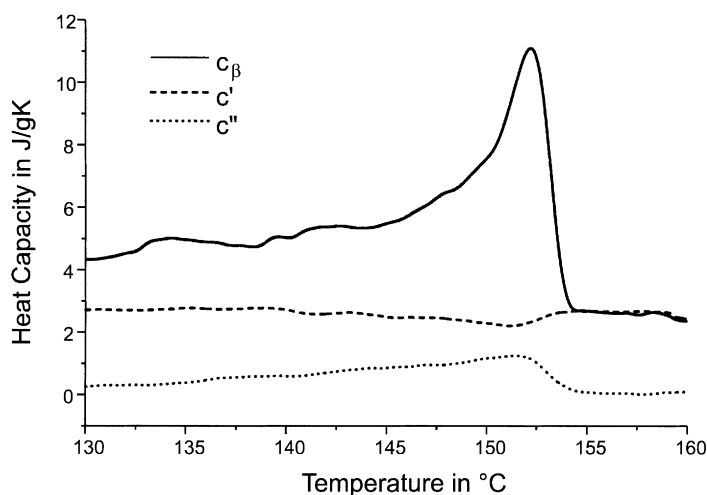


**Figure 1** TMD.s.c. curves ( $c_\beta$ ,  $c'$  and  $c''$ ) obtained for s-PP during a heating subsequent to a crystallization (3 h) at  $130^\circ\text{C}$  ( $\beta_0 = 0.5 \text{ K min}^{-1}$ ,  $f = 14 \text{ mHz}$ ,  $T_a = 0.1 \text{ K}$ )

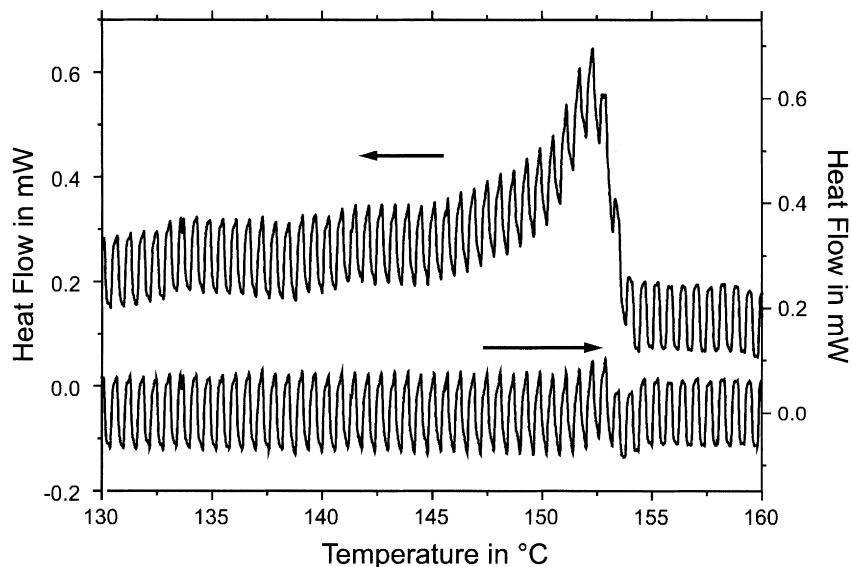


**Figure 2** Same measurement as Fig.1. Total heat flow  $\Phi$  and periodic component of the heat flow  $\Phi_p$ .  $\Phi_p$  is calculated as the difference between  $\Phi$  and its average over one period

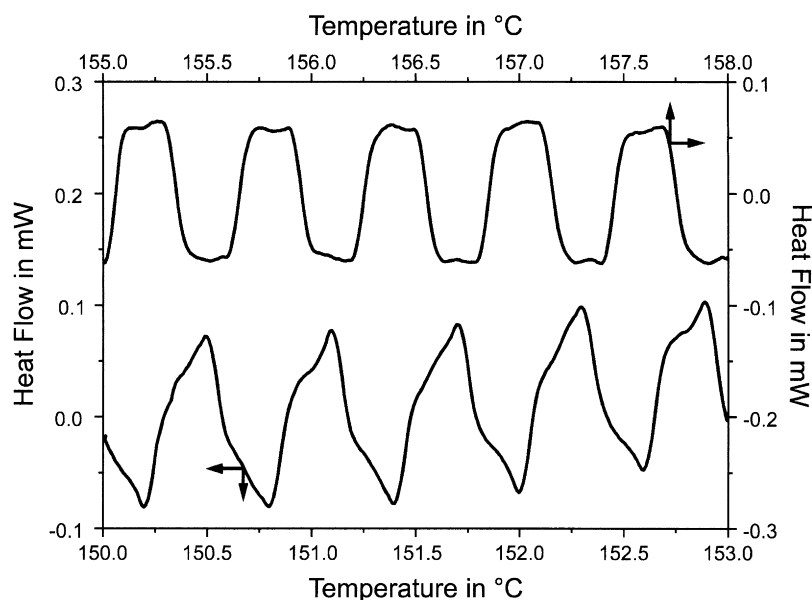


**Figure 3**  $\Phi_p$  from Fig.2 in the region of the melting peak (lower curve) and in the melt (upper curve)

signal. As is observed, the  $\Phi_p$ -signal in the melt has such a shape. On the other hand, in the melting region deviations occur. To see the formal background of the modification, calculations were carried out. A rectangular-shaped periodic heat flow can be described by a series of the odd-numbered harmonics

$$\Phi_p = \frac{4}{\pi} \Phi_a \left( \cos(\omega t - \phi_1) - \frac{\cos(3\omega t - \phi_3)}{3} + \frac{\cos(5\omega t - \phi_5)}{5} - \dots \right) \quad (4)$$

whereby all phases are equal. The continuous line in *Figure 4* represents this result (calculation up to the 15th harmonics and smoothing within a window  $d(\omega t) = 0.2$ ). The curve drawn with a broken line is obtained when choosing for the phase of the first harmonic the value  $\phi_1 = 0.6$ . Comparison of *Figures 3 and 4* shows, that this essentially

reproduces the experimental result. Note that the symmetry of the temperature variation is retained in  $\Phi_p$ . Hence, also here, there are no indications for non-linear effects.

Finally we determined all Fourier components of  $\Phi_p$  for the complete curve through all temperatures. *Figure 5* shows the moduli up to the 13th harmonic. As expected from the symmetry only odd-numbered harmonics are detected. The peak amplitudes in *Figure 5* are smaller than expected theoretically. This is caused by the phase shift of the first harmonic in the melting region and probably also by heat-transfer effects.

#### Theoretical considerations

As demonstrated by the results of *Figure 1*, the melting shows up in the complex heat capacity. Observations are indicative for the occurrence of reversible melting-crystallization processes at the crystal surfaces<sup>4,6,8,13</sup>. The TMD.s.c. experiment is sensible for such local processes.

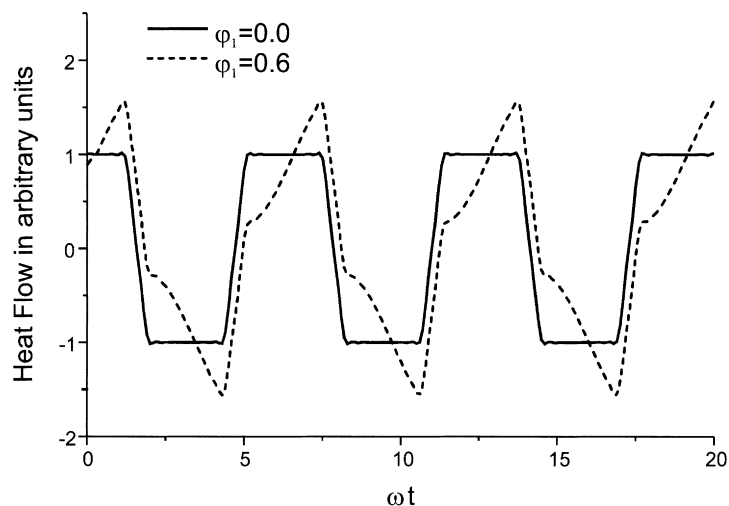


Figure 4 Simulated heat flow curve obtained with equation (4), for zero phase shifts (solid curve) and with a phase shift in the 1st harmonic of 0.6 (dashed curve)

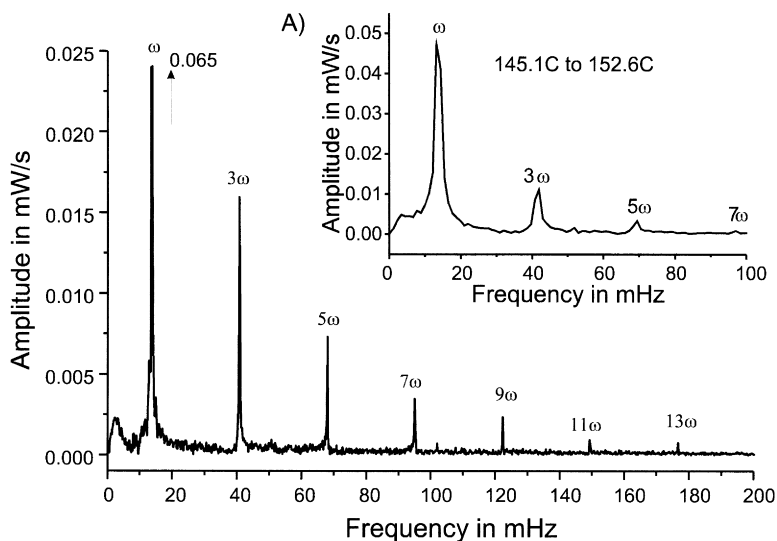


Figure 5 Fourier transform of the heat flow ( $\Phi(t)$ ) shown in Fig.2. (A) Fourier transform of the heat flow ( $\Phi(t)$ ) in the region of the melting peak (145.1°C–152.6°C)

If the rate of local melting rate varies linearly with the temperature, a contribution to  $c''$  arises. In order to account for the  $c'$ -signal, an additional relaxation process causing a time-dependent change of the melting rate subsequent to a temperature step must be introduced<sup>13</sup>. Such local relaxation processes may well take place in the melt close to the crystal surface, with characteristic times in the order of the period of the temperature variation. In this paper we shall not further discuss this phenomenon and restrict the discussion to the imaginary part of the complex heat capacity, under neglect of any memory and relaxation effects.

We describe the time-dependent changes in the crystallinity  $\alpha$  with the aid of an order parameter  $\zeta$ , introduced by

$$\alpha(t) = \alpha_{\max} \zeta(t) \quad (5)$$

Here  $\alpha_{\max}$  denotes the crystallinity at the end of isothermal crystallization.

The rate of transformation

$$\dot{\zeta} = \frac{d\zeta}{dt} \quad (6)$$

gives a contribution to the total heat flow:

$$\Phi(t) = mc_p \beta(t) + m \Delta h_f \dot{\zeta}(t) \quad (7)$$

Here  $\Delta h_f$  is the melting enthalpy per unit mass and  $m$  the sample mass. Generally, the melting rate depends on the superheating of a crystal. Signals arise from those crystals which have their equilibrium melting point,  $T_f$ , near to the mean temperature. For the variation of the melting rate associated with the periodic temperature fluctuation, one can assume a linear dependence on the superheating  $T - T_f$ :

$$\dot{\zeta}(T) = \left( \frac{d\dot{\zeta}}{dT} \right)_{T_f} (T - T_f) \quad (8)$$

equation (7) yields the melting curve in conventional d.s.c. measurements. It follows as

$$c_\beta - c_p = c_m = \frac{\delta h_f \dot{\zeta}}{\beta_0} \quad (9)$$

i.e. by a subtraction of the baseline given by the true heat capacity of the sample.

In the TMD.s.c. experiment the first harmonic of the periodic component of the temperature program reads

$$T_p(t) = T_a \sin(\omega t) \quad (10)$$

equation (7) and (8) give the periodic component of the heat flow

$$\Phi_p(t) = mc_p T_a \omega \cos(\omega t) + m \Delta h_f \left( \frac{d\dot{\zeta}}{dT} \right) T_a \sin(\omega t) \quad (11)$$

On the other hand, the periodic heat flow reads

$$\Phi_p(t) = mc'_p T_a \omega \cos(\omega t) + mc'' T_a \omega_0 \sin(\omega t) \quad (12)$$

A comparison of equation (11) and equation (12) yields

$$c'' = \frac{\Delta h_f \left( \frac{d\dot{\zeta}}{dT} \right)}{\omega} \quad (13)$$

From equation (9) and equation (13) follows

$$\frac{c''}{c_m} = \frac{\beta_0 \left( \frac{d\dot{\zeta}}{dT} \right)}{\omega \dot{\zeta}} \quad (14)$$

and using equation (8) one gets

$$\frac{c''}{c_m} = \frac{\beta_0}{\omega(T - T_f)} \quad (15)$$

Since

$$\int_{\text{Peak}} c_m(T) dt = \delta h_f \quad (16)$$

we finally arrive at

$$\frac{\omega}{\beta_0} \int_{\text{Peak}} c'' dT = \frac{\Delta h_f}{\langle T - T_f \rangle} \quad (17)$$

Melting of a crystallite starts when  $T = T_f$  and then increases up to the point of complete fusion. The superheating increases correspondingly and we, therefore, have to introduce into the equation the average  $\langle T - T_f \rangle$ .

equation (17) shows that the area of the  $c''$ -peak depends on the superheating. At a given frequency this area is proportional to  $1/\langle T - T_f \rangle$ . Because the superheating should be independent of the frequency, it follows that  $\omega$  times the peak area should be a constant.

The amount of superheating depends on  $\beta_0$ . From equation (8) follows for the maximum melting rate

$$\dot{\zeta}_{\text{max}} = \left( \frac{\partial \dot{\zeta}}{\partial T} \right)_{T_f} \beta_0 \Delta t_f \quad (18)$$

where  $\Delta t_f$  is the total time required for a crystallite melting. Because the melting rate is a linear function of time or temperature the average melting rate is

$$\langle \dot{\zeta} \rangle = \frac{\dot{\zeta}_{\text{max}}}{2} \quad (19)$$

Correspondingly the average superheating and  $\Delta t_f$  are related by

$$\langle T - T_f \rangle = \frac{\beta_0 \Delta t_f}{2} \quad (20)$$

$\Delta t_f$  depends on the volume of a crystal. As the melting rate increases linearly we have

$$\nu_c = \text{const.} \left( \frac{\partial \dot{\zeta}}{\partial T} \right)_{T_f} \frac{\beta_0}{2} \Delta t_f^2 \quad (21)$$

This means that  $\Delta t_f$  changes with the heating rate as

$$\Delta t_f \propto \frac{1}{\sqrt{\beta_0}} \quad (22)$$

The relation between the average superheating and the underlying heating rate follows from equation (20) and equation (22):

$$\langle T - T_f \rangle = A \sqrt{\beta_0} \quad (23)$$

where  $A$  is a constant.

Hence, as shown by these considerations, evaluation of the  $c''$ -peak yields the average superheating. In addition, a linear relationship between  $\langle T - T_f \rangle$  and the square root of the underlying heating rate is predicted. Our experiments allow for a check.

## EXPERIMENTAL RESULTS

We started with a check of the frequency dependence of the complex heat capacity using a series of frequencies between 10 mHz and 42 mHz. The temperature amplitude was 0.1 K

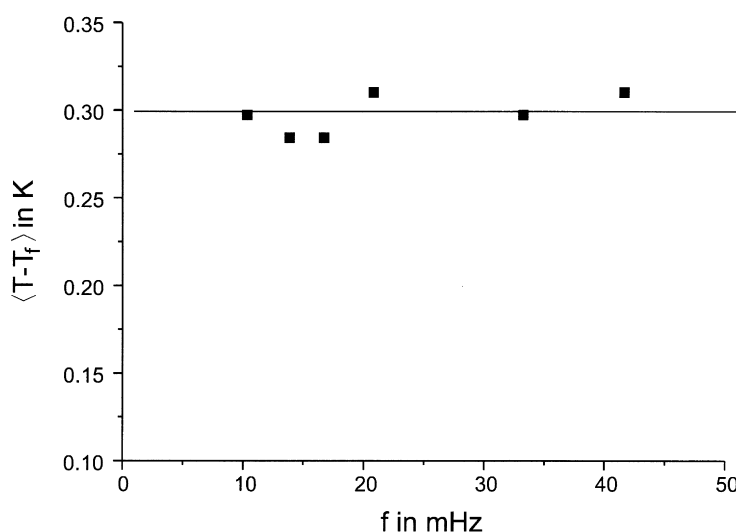


Figure 6 Superheating as a function of frequency ( $T_a$ , 0.1 K;  $\beta_0$ , 0.5 K min<sup>-1</sup>)

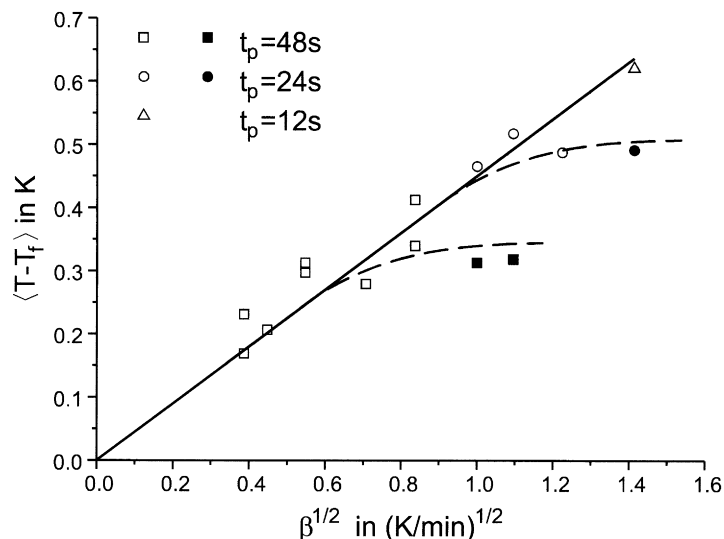


Figure 7 Superheating as a function of the square root of the underlying heating rate obtained at different frequencies

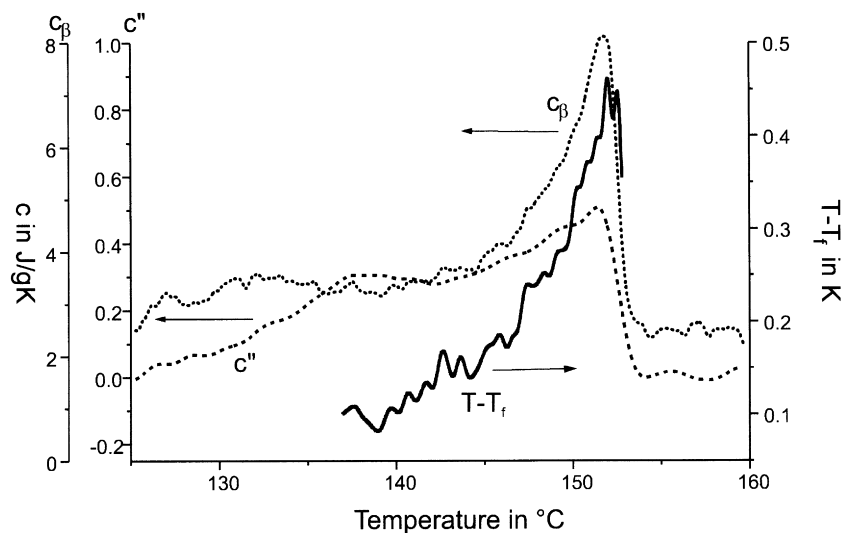


Figure 8  $c_{\beta}, c''$  and superheating as function of temperature in the melting range ( $T_a, 0.1\text{ K}$ ;  $\beta_0, 0.3\text{ K min}^{-1}$ ;  $f, 21\text{ mHz}$ )

and the underlying heating rate  $0.5\text{ K min}^{-1}$ .  $\Delta h_f$  was determined by conventional d.s.c., giving  $53\text{ J g}^{-1}$ . Then  $\langle T - T_f \rangle$  was derived from the area under the  $c''$ -signal using equation (17). The result is shown in Figure 6. As we see, the superheating obtained is indeed frequency independent. This implies that the intensity of the  $c''$ -signal, when referred to the underlying averaged melting curve, decreases linearly with the applied frequency.

In order to check the dependence of the superheating on the underlying heating rate as given by equation (23), the heating rate was varied between  $0.15$  and  $2.5\text{ K min}^{-1}$  ( $T_a = 0.1\text{ K}$ ). The results are depicted in Figure 7. For a frequency of  $21\text{ mHz}$  (period  $t_p = 48\text{ s}$ ), the determined superheating shows the expected linear dependence up to an underlying heating rate of  $0.8\text{ K min}^{-1}$ . For the higher  $\beta_0$ s (filled symbols) the experimental results are systematically too low. The reason is that the change of the underlying average temperature during one period reaches at  $0.8\text{ K min}^{-1}$  a critical limit of  $0.6\text{ K}$ . In this case the prerequisites for a decomposition of the total heat flow rate into an underlying and a periodic component are no longer fulfilled<sup>14</sup>. If the frequency is changed to  $42\text{ mHz}$  ( $t_p = 24\text{ s}$ ), the superheating follows the linear dependence up to  $\beta_0 = 1.3$

$\text{K min}^{-1}$ , where again the critical limit is reached. Finally, we used a frequency of  $83\text{ mHz}$ . Now a linear dependence is observed up to the highest used heating rates. Hence, the predictions of the model with regard to the effects of frequency and heating rate are verified experimentally, which gives us trust into the values deduced for the superheating.

Rather than deriving one value of the superheating for the whole melting range, one can also obtain it as a function of temperature, when applying equation (15). The results are presented in Figure 8, being obtained for  $\beta_0 = 0.3\text{ K min}^{-1}$ ,  $f = 21\text{ mHz}$  and  $T_a = 0.1\text{ K}$ . The largest superheating is found at the melting peak and amounts to  $0.46\text{ K}$ . According to our discussion, for a constant underlying heating rate the superheating can be related to the volume of the crystallites. Therefore, one might understand the observation as indicating that the crystallites which melt at lower temperatures are smaller. Figure 9 demonstrates once again the influence of the heating rate, now in temperature resolved curves. One observes a general increase on increasing  $\beta_0$ . The superheating at the melting peak can also be determined directly in a conventional d.s.c. run by measuring the shift of the peak location as a function of  $\beta_0$ .

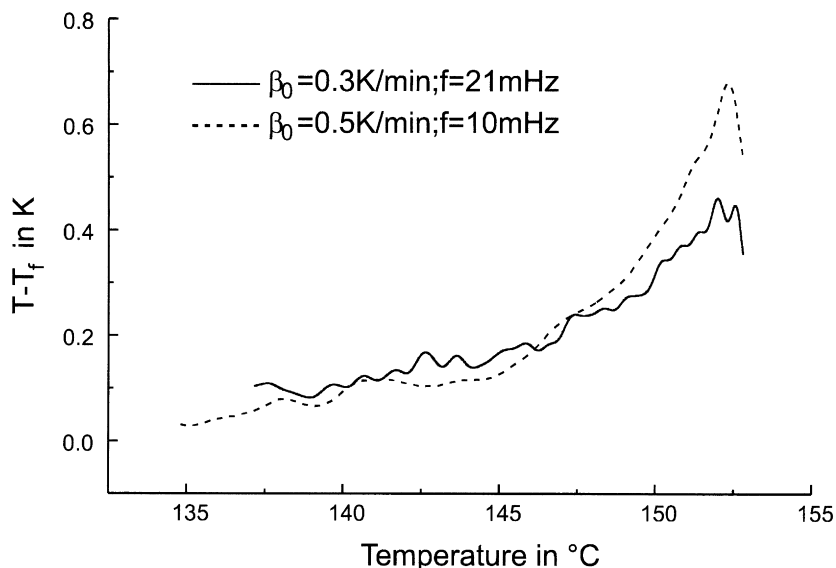


**Figure 9** Superheating as a function of temperature measured under the indicated conditions

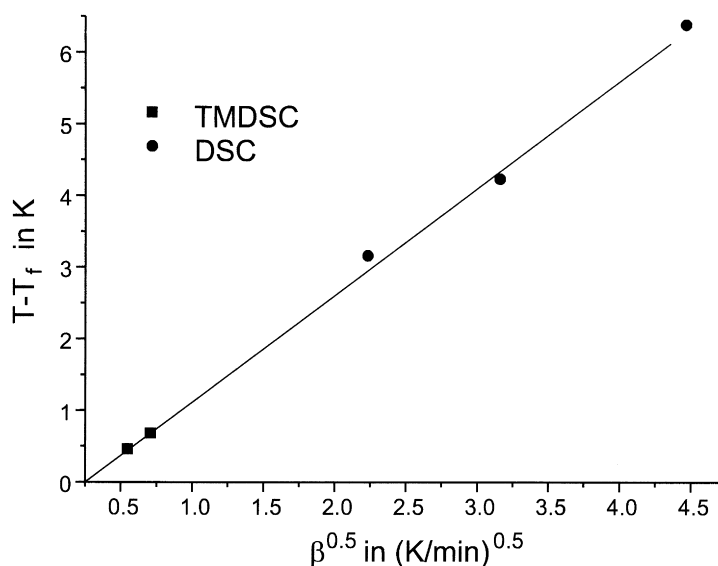


**Figure 10** Superheating at the peak position as a function of the square root of the heating rate in a comparison of results from TMDSC and conventional DSC.

In *Figure 10* we compare the maximum values in *Figure 9* with those obtained by conventional DSC, using heating rates of 5, 10 and 20 K min<sup>-1</sup> and correcting the data for heat transfer effects. We observe a good agreement between the two independent determination methods.

#### ACKNOWLEDGEMENTS

The authors gratefully acknowledge the help of E. Bergmann (IFA GmbH, Ulm) during the measurements and the support by the Perkin-Elmer Corporation.

#### REFERENCES

1. Wunderlich, B., *Macromolecular Physics*, Vols 1, 2, 3. Academic Press, New York, 1973.
2. Strobl, G., *The Physics of Polymers*, Chap. 4. Springer, Berlin, 1996.
3. Reading, M., *Trends in Polymer Sci.*, 1993, **8**, 248.
4. Okazaki, I. and Wunderlich, B., *Macromolecules*, 1997, **30**, 1758.
5. Wurm, A., Merzlyakov, M. and Schick, C., *Colloid and Polym. Sci.*, 1997, **00**, 000.
6. Toda, A., Oda, T., Hikosaka, M. and Surayama, Y., *Polymer*, 1997, **38**, 231.
7. Toda, A., Tomota, C., Hikosaka, M. and Surayama, Y., *Polymer*, 1997, **38**, 2849.
8. Schmidtke, J., Strobl, G. and Thurn-Albrecht, T., *Macromolecules*, 1997, **00**, 00.
9. Thomann, R., Wang, C., Kressler, J., Jüngling, S. and Mühlhaupt, R., *Polymer*, 1995, **36**, 3795.
10. Schawe, J.E.K. and Höhne, G.W.H., *Thermochim. Acta*, 1996, **287**, 213.
11. Schawe, J.E.K. and Winter, W., *Thermochim. Acta*, 1997, **298**, 9.
12. Weyer, S., Hensel, A. and Schick, C., *Thermochim. Acta*, 1997.
13. Schawe, J.E.K. and Bergmann, E., *Thermochim. Acta*, 1997.
14. Schawe, J.E.K., *Thermochim. Acta*, 1996, **271**, 127.